Supporting information for:

A Mn(III) single ion magnet with tridentate Schiff-base ligands

S. Realista,[a] A. J. Fitzpatrick,[b] G. Santos,[a] L. P. Ferreira,[c,d] S. Barroso,[e] L. C. J. Pereira,[f] N. A. G. Bandeira,[a,g]

P. Neugebauer,[h] J. Hrubý,[h] G. G. Morgan,[b] J. van Slageren,[h] M. J. Calhorda[a] and P. N. Martinho*[a]

a Centro de Química e Bioquímica, Faculdade de Ciências, Universidade de Lisboa, Campo Grande, 1749-016 Lisboa, Portugal E-mail: pnmartinho@ciencias.ulisboa.pt
b School of Chemistry, University College Dublin, Belfield, Dublin 4, Ireland
c BioISI, Faculdade de Ciências, Universidade de Lisboa, Campo Grande, 1749-016 Lisboa, Portugal
d Department of Physics, University of Coimbra, 3004-516 Coimbra, Portugal
e Centro de Química Estrutural, Instituto Superior Técnico, Universidade de Lisboa
Av. Rovisco Pais, 1049-001 Lisboa, Portugal
f C2TN, Centro de Ciências e Tecnologias Nucleares, Instituto Superior Técnico, Universidade de Lisboa, Estrada Nacional 10, ao Km 139,7, 2695-066 Bobadela LRS, Portugal
g Institute of Chemical Research of Catalonia (ICIQ), Avda. Països Catalans, 16- 43007 Tarragona, Spain
h Institut für Physikalische Chemie, Universität Stuttgart Pfaffenwaldring 55, 70569 Stuttgart, Germany

Contents

1. Detailed structural data

Table S1 Selected crystallographic experimental data and structure refinement parameters for complex **1**.

|	**1**
Empirical formula	$C_{50}H_{58}BMnN_4O_4$
Formula weight	844.75
Temperature (K)	150(2)
Crystal system	Monoclinic
Space group	$P2_1/n$
a(Å)	12.066(1)
b(Å)	18.279(1)
c(Å)	20.890(1)
α(°)	90
β(°)	91.47(0)
γ(°)	90
V(Å^3)	4605.9(4)
Z, ρ_{calc} (g cm^{-3})	4, 1.218
μ(mm^{-1})	0.334
Crystal size	0.5×0.4×0.2
Crystal colour	red
Crystal shape	prism
Refl. collected	64095
Unique refl. [R(int)]	11471 [0.0356]
R1 [I>2σ(I)]	0.0346
wR2 [I>2σ(I)]	0.0891
GooF	1.054

Complex **1** crystallises in the monoclinic system, space group $P2_1/n$, with two half [Mn(3-OEt-salme)$_2$]$^+$ cations and one BPh$_4^-$ anion in the asymmetric unit. Although crystallographically independent, the two cations have very similar parameters. Selected bond distances and angles (data obtained at 150 K) are listed in Table S2.

Table S2 Selected bond lengths (Å) and angles (°) for complex **1** (*cations 1* and *2*).[a]

	cation 1	*cation 2*
Mn(1)-O(2); Mn(1)-O(2)#	1.8663(8)	1.8745(8)
Mn(1)-N(1); Mn(1)-N(1)#	2.0286(10)	2.0342(10)
Mn(1)-N(2); Mn(1)-N(2)#	2.3434(10)	2.3551(11)
O(2)#-Mn(1)-O(2)	180	180
N1(1)-Mn(1)-N(1)#	180	180
O(2)-Mn(1)-N(1); O(2)#-Mn(1)-N(1)#	88.66(4)	88.73(4)
O(2)#-Mn(1)-N(1); O(2)-Mn(1)-N(1)#	91.34(4)	91.27(4)
O(2)-Mn(1)-N(2); O(2)#-Mn(1)-N(2)#	89.28(4)	89.30(4)
O(2)#-Mn(1)-N(2); O(2)-Mn(1)-N(2)#	90.72(4)	90.70(4)
N(1)-Mn(1)-N(2)#; N(1)#-Mn(1)-N(2)	97.69(4)	98.08(4)
N(1)-Mn(1)-N(2); N(1)#-Mn(1)-N(2)#	82.31(4)	81.92(4)

[a]Equivalent atoms labelled with # are generated using the symmetry transformation -x,-y,-z for *cation 1* and -x,-y+1,-z for *cation 2*.

The crystal packing of complex **1**, depicted in Figure S1, shows alternating layers of the Mn(III) cations and BPh$_4^-$ anions parallel to the *ab* plane. The layers are interconnected through short intermolecular contacts between neighbouring cations and anions.
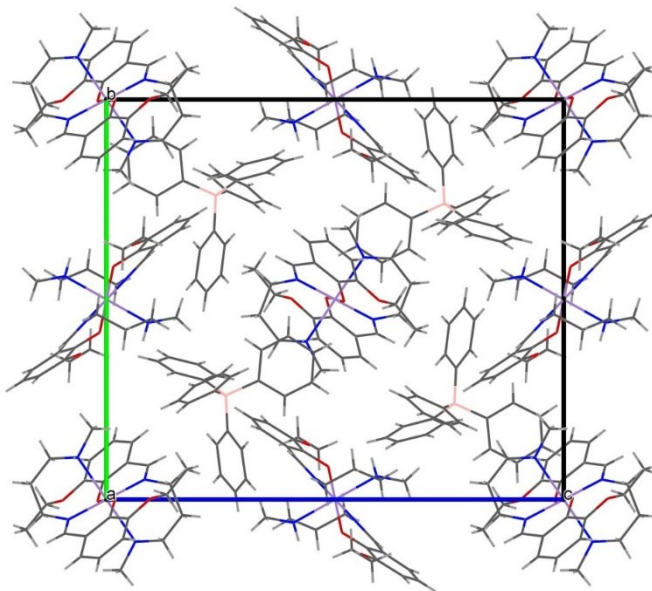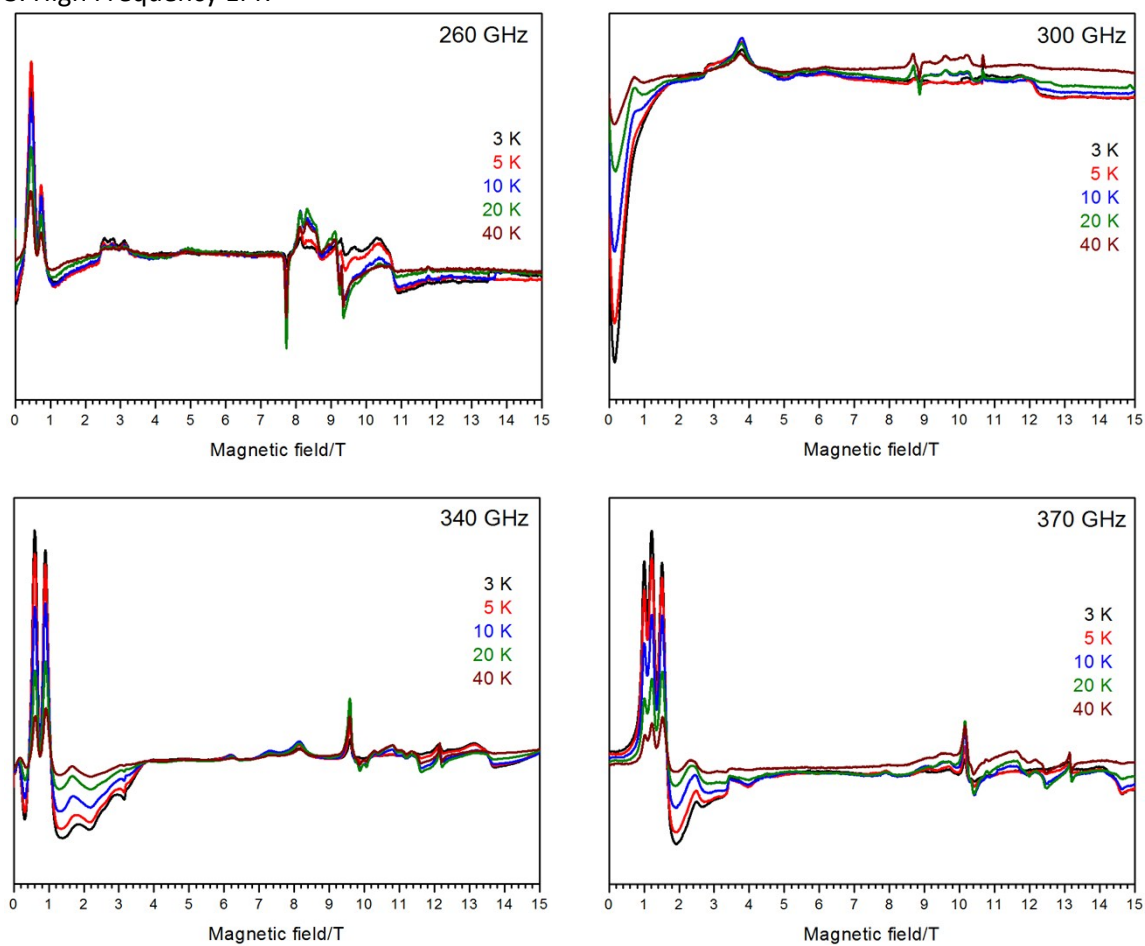

Figure S1 Mercury packing diagram of complex **1** viewed along the *a* axis.
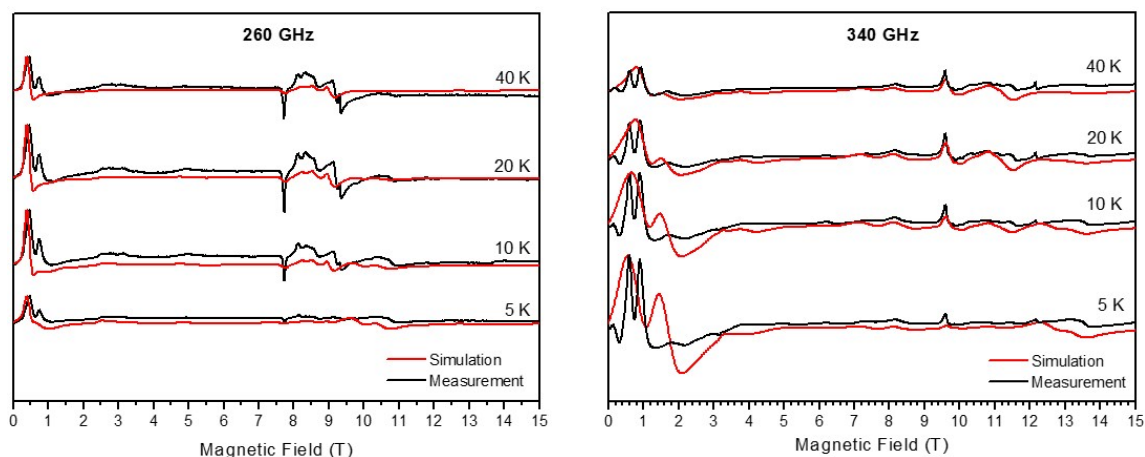
2. Magnetic data
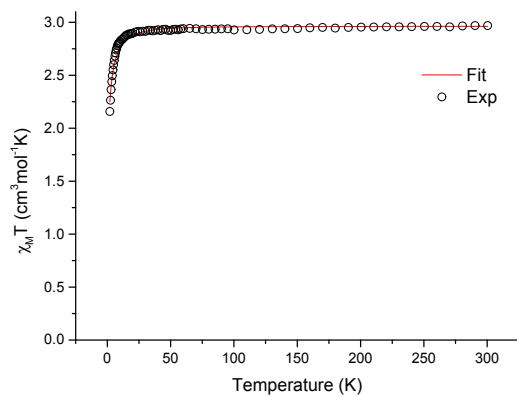
Figure S2 Temperature variation of the $\chi_M T$ product, where χ_M is the molar susceptibility and T is the temperature. Fit according to Eqn. 1, see main article text for details.

3. High Frequency EPR

Figure S3. High Frequency EPR spectra of compressed powder recorded at various frequencies and teperatures as indicated in the plot.

Figure S4. High Frequency EPR spectra (in black) of compressed powder recorded at 260 GHz and 340 GHz frequencies and various teperatures as indicated in the plot, together with simulation (in red) obtained using parameters indicated in Table 1.

4. AC Magnetisation
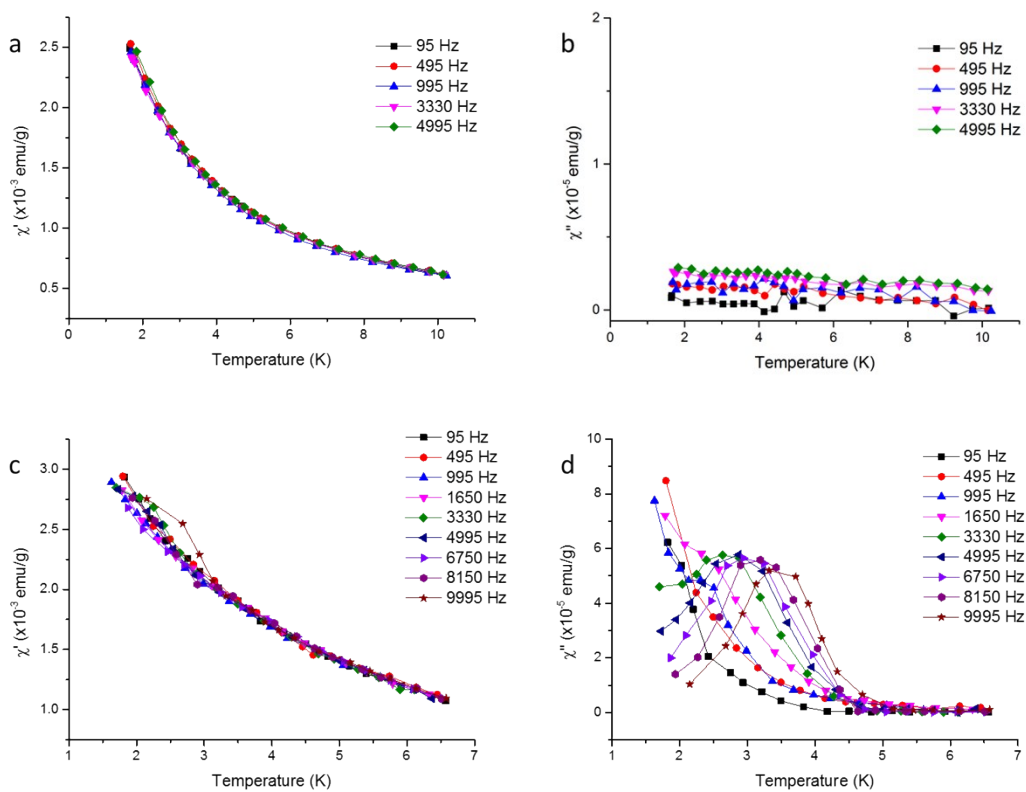
Figure S5 AC magnetisation of complex **1**; a) χ' under 0 *Oe* DC field; b) χ'' under 0 *Oe* DC field; c) χ' under 2000 *Oe* DC field; d) χ'' under 2000 *Oe* DC field.

Table S3 Generalised Debye model fitting parameters from 1.6 to 4 K for complex **1**.

T (K)	χ_S	χ_T	α	τ
1.6	0.00285	0.00313	0.24717	2.94707E-4
2.0	0.0022	0.00244	0.15953	2.21434E-4
2.2	0.00216	0.00235	0.05117	1.57822E-4
2.4	0.00201	0.00216	0.0421	1.09633E-4
2.6	0.00192	0.00205	0.25818	7.69267E-5
3.0	0.00181	0.00188	0.3011	4.38904E-5
3.4	0.00164	0.00178	0.53571	2.86637E-5
3.6	0.00162	0.00171	0.40644	2.3774E-5
4.0	0.00154	0.00162	0.41684	1.93699E-5

5. Computational data

The zero field splitting (ZFS) phenomenon in a mononuclear transition metal complex can be described by the multispin Hamiltonian[1]

$$\hat{H}_{ZFS} = \hat{S}\mathbf{D}\hat{S} \qquad \backslash* \text{ MERGEFORMAT (1)}$$

in which **D** is the tensor describing the ZFS. Within the magnetic axes frame **D** can be made traceless and shifted by a constant value such that in cubic symmetry $D_{XX}=D_{YY}=D_{ZZ}$ and D=0. Z will be, by convention, the most different axis of magnetisation with respect to all the rest which is to say either the hard (D>0) or the easy (D<0) axis. Additionally X will be the intermediate axis of magnetisation such that $D_{XX}-D_{YY}=2E>0$. In this manner the magnetic axes frame and the ZFS parameters are defined univocally as:

$$\hat{H}_{ZFS} = D\left[\hat{S}_Z^2 - \frac{1}{3}S(S+1)\right] + E\left(\hat{S}_X^2 - \hat{S}_Y^2\right)$$

$$D \equiv \frac{3}{2}\mathbf{D}_{ZZ}, E \equiv \frac{1}{2}(\mathbf{D}_{XX} - \mathbf{D}_{YY})$$

$\backslash*$ MERGEFORMAT (2)

Here D and E are scalar numbers the latter being the rhombic ZFS. Since a Mn(III) centre has a $3d^4$ electron count the ZFS Hamiltonian can be expressed[2] as

M_S	$\lvert-2\rangle$	$\lvert-1\rangle$	$\lvert 0\rangle$	$\lvert+1\rangle$	$\lvert+2\rangle$
$\langle-2\rvert$	$2D$	0	$\sqrt{6}E$	0	0
$\langle-1\rvert$	0	$-D$	0	$3E$	0
$\langle 0\rvert$	$\sqrt{6}E$	0	$-2D$	0	$\sqrt{6}E$
$\langle+1\rvert$	0	$3E$	0	$-D$	0
$\langle+2\rvert$	0	0	$\sqrt{6}E$	0	$2D$

$\backslash*$ MERGEFORMAT (3)

The rhombic factor E comes up when mixing spin-orbit coupled states that differ by $M_s\pm2$.

Since calculations of ZFS parameters necessarily involve spin-orbit coupling (SOC) and, therefore, a linear combination of spin states which are themselves based in atomic orbitals (not momentum functions), a transformation into the basis set of momentum functions will eventually be required. This implies that the ZFS Hamiltonian matrix will be a set of complex values, only the real part being displayed in (3). The D and E parameters will however be real numbers.

Table S4 Complex MOLCAS/CAS(4,5) spin-orbit Hamiltonian in the basis of pseudo-spin eigenfunctions of the quintet state manifold.

	$\left|-2\right\rangle$	$\left|-1\right\rangle$	$\left|0\right\rangle$	$\left|+1\right\rangle$	$\left|+2\right\rangle$
$\left\langle-2\right|$	-6.426	-0.00700+0.435i	+1.590-0.00290i	$+2.3\times10^{-4}+0.00104i$	$-0.0139+2.2\times10^{-4}i$
$\left\langle-1\right|$	-0.00700-0.435i	+3.213	-0.00275+0.177i	+1.945-0.00316i	$-2.3\times10^{-4}-0.00104i$
$\left\langle0\right|$	+1.590+0.00290i	-0.00275-0.177i	+6.426	+0.00275-0.177i	+1.590-0.00290i
$\left\langle+1\right|$	$+2.3\times10^{-4}-0.00104i$	+1.945+0.00316i	+0.00275+0.177i	+3.213	+0.00700-0.435i
$\left\langle+2\right|$	$-0.0139-2.2\times10^{-4}i$	$+2.3\times10^{-4}+0.00104i$	+1.590+0.00290i	+0.00700+0.435i	-6.426

Zero Field Splitting Hamiltonian (cm-1)
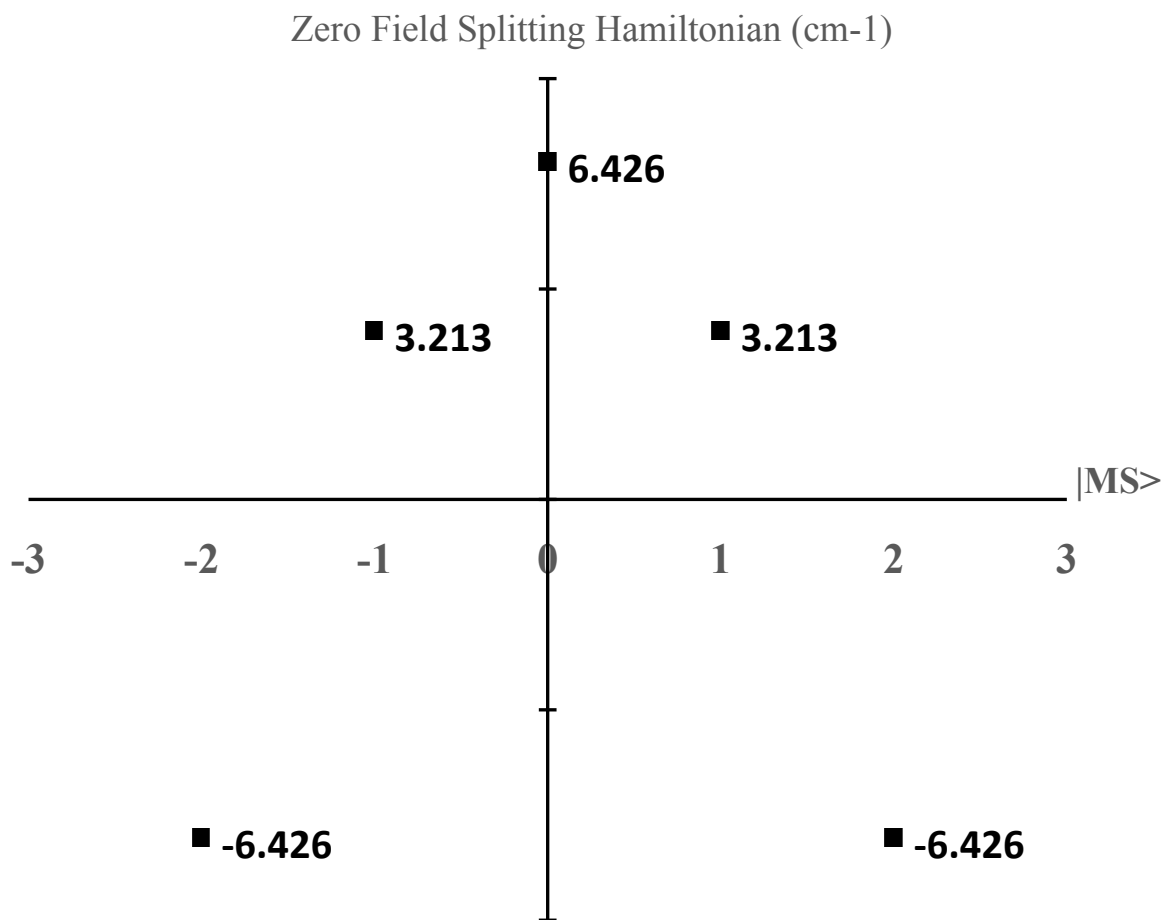
Figure S6 Real part of the ZFS Hamiltonian diagonal of unit A [CAS(4,5)SCF+SOC] in the basis of pseudo-spin momentum functions.
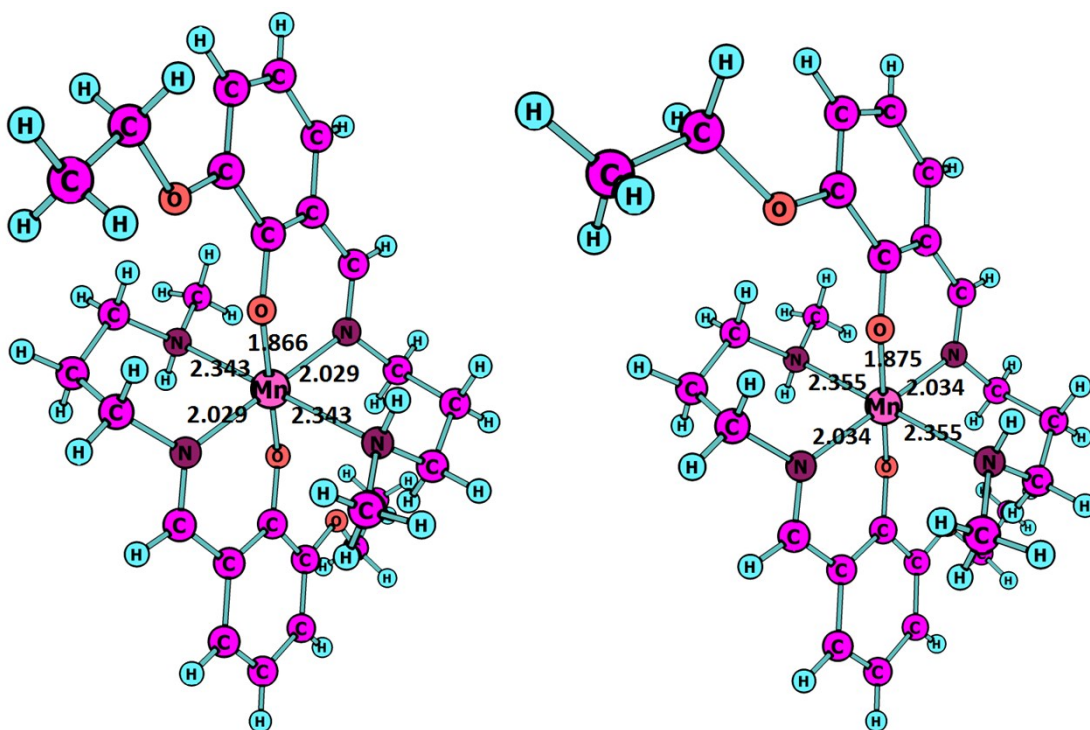
Figure S7 Unit A (left) and unit B (right) with the most significant bond lengths in Å.

Table S5 ORCA/CASSCF spin-orbit coupled states and their major contributions (%) in the basis of spin momentum components.

Quintet components	E(cm⁻¹)	$\|M_s=-2\rangle$	$\|M_s=-1\rangle$	$\|M_s=0\rangle$	$\|M_s=+1\rangle$	$\|M_s=+2\rangle$
SOC State 1	0	6.3		87.0		6.3
SOC State 2	0.354		49.9		49.9	
SOC State 3	7.751		49.8		49.8	
SOC State 4	11.26	49.9				49.9
SOC State 5	12.88	43.6		12.6		43.6

Table S6 NEVPT2 spin-orbit coupled states and their major contributions (%) in the basis of spin momentum components.

Quintet components	E(cm⁻¹)	$\|M_s=-2\rangle$	$\|M_s=-1\rangle$	$\|M_s=0\rangle$	$\|M_s=+1\rangle$	$\|M_s=+2\rangle$
SOC State 1	0	4.4		90.7		4.4
SOC State 2	0.868		49.8		49.8	
SOC State 3	9.134		49.8		49.8	
SOC State 4	15.41	49.9				49.9
SOC State 5	16.90	45.5		8.79		45.5

6. References

1. J. P. Launay and M. Verdaguer, *Electrons in Molecules: From Basic Principles to Molecular Electronics*, OUP Oxford, 2013.
2. R. Boča, *Theoretical Foundations of Molecular Magnetism*, Elsevier Science, 1999.